10. Burger, A. M. *et al.* Effect of oncogene expression on telomerase activation and telomere length in human endothelial, fibroblast and prostate epithelial cells. *Int. J. Oncol.* **13,** 1043–1048 (1998).
11. Flore, A. *et al.* Transformation of primary human endothelial cells by Kaposi's sarcoma-associated herpesvirus. *Nature* **394,** 588–592 (1998).
12. Nakamura, T. M. & Cech, T. R. Reversing time: origin of telomerase. *Cell* **92,** 587–590 (1998).
13. Kipling, D. Telomere structure and telomerase expression during mouse development and tumorigenesis. *Eur. J. Cancer* **33,** 792–800 (1997).
14. Kim, N. W. *et al.* Specific association of human telomerase activity with immortal cells and cancer. *Science* **266,** 2011–2015 (1994).
15. Shay, J. W. & Bacchetti, S. A survey of telomerase activity in human cancer. *Eur. J. Cancer* **33,** 787–791 (1997).
16. Harley, C. B. *et al.* Telomerase, cell immortality, and cancer. *Cold Spring Harb. Symp. Quant. Biol.* **59,** 307–315 (1994).
17. Bodnar, A. G. *et al.* Extension of life-span by introduction of telomerase into normal human cells. *Science* **279,** 349–352 (1998).
18. Kiyono, T. *et al.* Both Rb/p16INK4a inactivation and telomerase activity are required to immortalize human epithelial cells. *Nature* **396,** 84–88 (1998).
19. Lustig, A. J. Crisis intervention: the role of telomerase. *Proc. Natl Acad. Sci. USA* **96,** 3339–3341 (1999).
20. Serrano, M., Lin, A. W., McCurrach, M. E., Beach, D. & Lowe, S. W. Oncogenic *ras* provokes premature cell senescence associated with accumulation of p53 nd p16ink4a. *Cell* **88,** 593–602 (1997).
21. Counter, C. M. *et al.* Dissociation among *in vitro* telomerase activity, telomere maintenance, and cellular immortalization. *Proc. Natl Acad. Sci. USA* **95,** 14723–14728 (1998).
22. Morales, C. P. *et al.* Absence of cancer-associated changes in human fibroblasts immortalized with telomerase. *Nature Genet.* **21,** 115–118 (1999).
23. Zalvide, J., Stubdal, H. & DeCaprio, J. A. The J domain of simian virus 40 large T antigen is required to functionally inactivate RB family proteins. *Mol. Cell. Biol.* **18,** 1408–1415 (1998).
24. Damania, B., Mital, R. & Alwine, J. C. Simian virus 40 large T antigen interacts with human TFIIB-related factor and small nuclear RNA-activating protein complex for transcriptional activation of TATA-containing polymerase III promoter. *Mol. Cell. Biol.* **18,** 1331–1338 (1998).
25. Reddel, R. R., Bryan, T. M. & Murnane, J. P. Immortalized cells with no detectable telomerase activity. A review. *Biochemistry (Mosc.)* **62,** 1254–1262 (1997).
26. Jiang, X.-R. *et al.* Telomerase expression in human somatic cells does not induce changes associated with a transformed phenotype. *Nature Genet.* **21,** 111–114 (1999).
27. Jat, P. S., Cepko, C. L., Mulligan, R. C. & Sharp, P. A. Recombinant retroviruses encoding simian virus 40 large T antigen and polyomavirus large and middle T antigens. *Mol. Cell. Biol.* **6,** 1204–1217 (1986).
28. Kim, N. W. & Wu, F. Advances in quantification and characterization of telomerase activity by the telomeric repeat amplification protocol (TRAP). *Nucleic Acids Res.* **25,** 2595–2597 (1997).
29. Cifone, M. A. & Fidler, I. J. Correlation of patterns of anchorage-independent growth with *in vivo* behavior of cells from a murine fibrosarcoma. *Proc. Natl Acad. Sci. USA* **77,** 1039–1043 (1980).
30. Feuer, G. *et al.* Potential role of natural killer cells in controlling tumorigenesis by human T-cell leukemia viruses. *J. Virol.* **69,** 1328–1333 (1995).

Acknowledgements. We thank M. Fleming for interpretation of tumour histology, J. Smith for the gift of early passage BJ fibroblasts, and S. Dessain, B. Elenbaas, D. Fruman, P. Steiner, S. Stewart and the members of Weinberg laboratory for helpful discussions and review of the manuscript. This work was supported in part by Merck and Co. (R.A.W.), the US NCI (R.A.W., A.S.L.), a Damon Runyon–Walter Winchell Cancer Research Foundation Postdoctoral Fellowship (W.C.H.), and a Human Frontiers Postdoctoral Fellowship (R.L.B.). C.M.C. is a Whitehead Scholar; W.C.H. is a Herman and Margaret Sokol postdoctoral fellow. R.A.W. is an American Cancer Society Research Professor and a Daniel K. Ludwig Cancer Research Professor.

Correspondence and requests for material should be addressed to R.A.W. (e-mail: weinberg@wi.mit.edu).

Essential role for oncogenic Ras in tumour maintenance

Lynda Chin*†‡, Alice Tam*†§, Jason Pomerantz§, Michelle Wong§, Jocelyn Holash‖, Nabeel Bardeesy†, Qiong Shen†, Ronan O'Hagan†, Joe Pantginis‖, Hao Zhou‖, James W. Horner II†, Carlos Cordon-Cardo¶, George D. Yancopoulos‖ & Ronald A. DePinho†#

† *Adult Oncology, Dana Farber Cancer Institute, Boston, Massachusetts 02115, USA*
‡ *Department of Dermatology, Harvard Medical School, Boston, Massachusetts 02115, USA*
# *Department of Medicine and Genetics, Harvard Medical School, Boston, Massachusetts 02115, USA*
§ *Albert Einstein College of Medicine, Bronx, New York 10461, USA*
¶ *Memorial Sloan Kettering Cancer Center, New York, New York 10021, USA*
‖ *Regeneron Pharmaceuticals, Tarrytown, New York 10591, USA*
* *These authors contributed equally to this work*

Advanced malignancy in tumours represents the phenotypic endpoint of successive genetic lesions that affect the function and regulation of oncogenes and tumour-suppressor genes[1]. The established tumour is maintained through complex and poorly understood host–tumour interactions that guide processes such as angiogenesis and immune sequestration. The many different genetic alterations that accompany tumour genesis raise questions as to whether experimental cancer-promoting mutations remain relevant during tumour maintenance. Here we show that melanoma genesis and maintenance are strictly dependent upon expression of H-Ras^{V12G} in a doxycycline-inducible H-Ras^{V12G} mouse melanoma model null for the tumour suppressor INK4a. Withdrawal of doxycycline and H-Ras^{V12G} down-regulation resulted in clinical and histological regression of primary and explanted tumours. The initial stages of regression involved marked apoptosis in the tumour cells and host-derived endothelial cells. Although the regulation of vascular endothelial growth factor (VEGF) was found to be Ras-dependent *in vitro*, the failure of persistent endogenous and enforced VEGF expression to sustain tumour viability indicates that the tumour-maintaining actions of activated Ras extend beyond the regulation of VEGF expression *in vivo*. Our results provide genetic evidence that H-Ras^{V12G} is important in both the genesis and maintenance of solid tumours.

a

Number of mice	Genotype Tyr–rtTA	Tet–Ras	INK4a	Doxycycline induction	Number of mice with melanoma	Latency (days ± s.d.)
40	+	+	–/–	Yes	10	60 ± 26
23	–	+	–/–	Yes	0	—
12	+	+	–/–	No	0	—

b

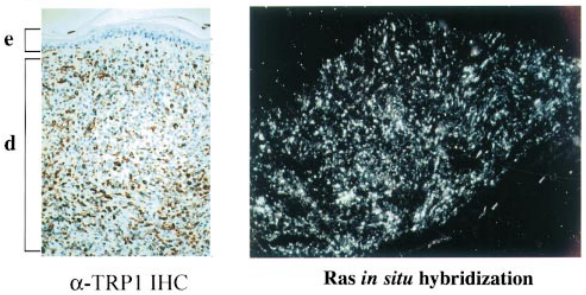

Figure 1 Inducible Tyr/Tet–Ras transgenic mice on INK4a-deficient background developed cutaneous melanomas. **a**, Summary of tumour incidence in the Tyr/Tet–Ras–INK4a-null colony and impact of doxycycline treatment. **b**, Left: anti-TRP1 staining of a primary cutaneous melanoma. Note strong immunoreactivity in dermal nodule with overlying intact epidermis; e, epidermis; d, dermis. Right: *in situ* hybridization for H-Ras^{V12G} transcript in a primary melanoma nodule.

To develop a cancer model in which dominantly acting oncoproteins are somatically regulated *in vivo*, transgenic mouse lines harbouring the reverse tetracycline transactivator[2] under the control of the tyrosinase gene promoter–enhancer elements (designated Tyr–rtTA) and another containing the H-Ras^{V12G} open reading frame driven by a minimal promoter containing multimerized tet-operons[2,3] (designated Tet–Ras) were inter-crossed with INK4a$^{+/-}$ mice to generate cohorts of single and double transgenic mice (designated Tyr/Tet–Ras) that were homozygous null for INK4a. Upon weaning, a subset of single and double transgenic INK4a$^{-/-}$ mice were given doxycycline in their drinking water[4]. In the doxycycline-treated group, 10 out of 40 Tyr/Tet–Ras INK4a$^{-/-}$ mice developed melanomas with an average latency of 60 days (Fig. 1a). In contrast, the untreated Tyr/Tet–Ras INK4a$^{-/-}$ mice ($n = 12$) or treated Tet–Ras INK4a$^{-/-}$ ($n = 23$) did not develop melanomas. The Tyr/Tet–Ras INK4a$^{-/-}$ melanomas shared all of the macroscopic features of the constitutive Tyr–Ras INK4a$^{-/-}$

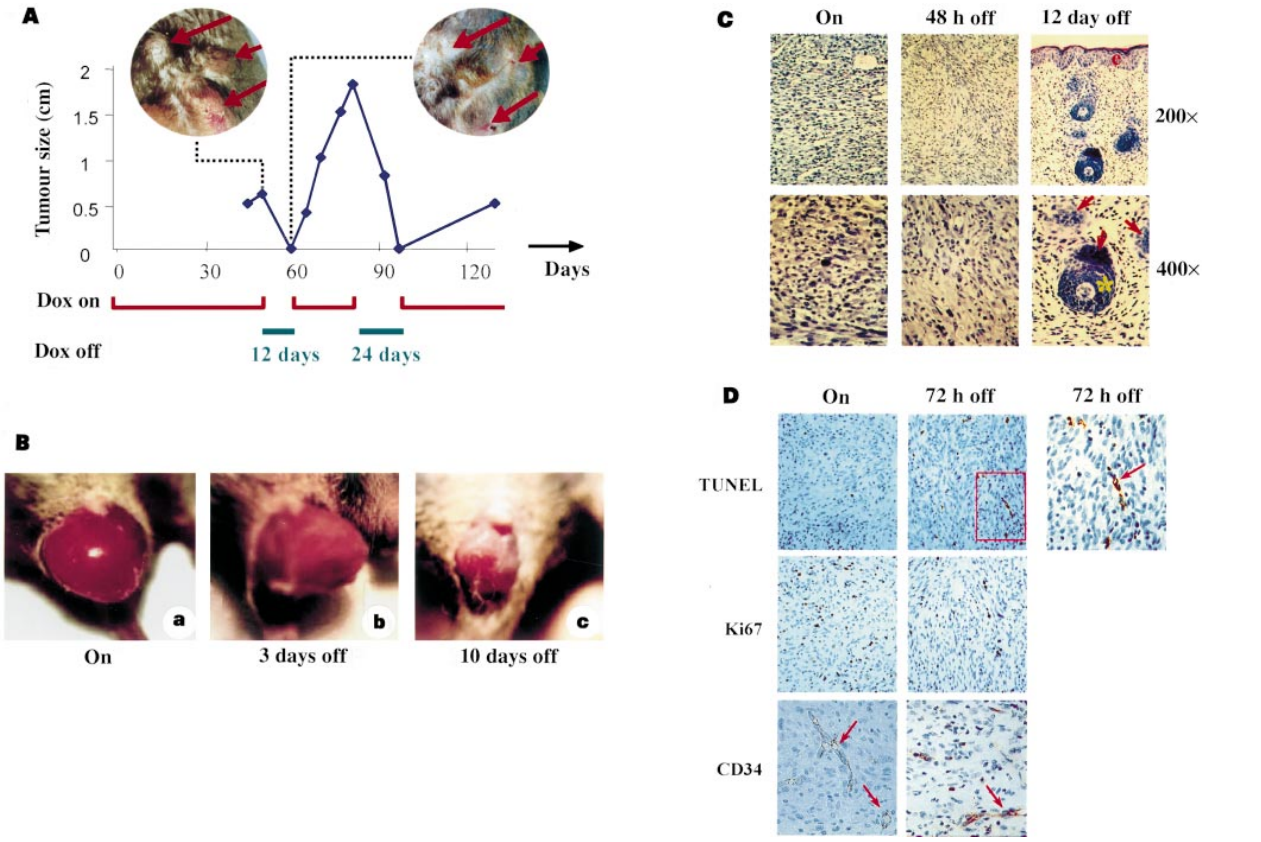

Figure 2 Activated Ras expression is necessary to maintain growth of established cutaneous melanomas *in vivo*. **A**, Tumour from R348 (Tet–Ras founder line 65) was measured at intervals and the longest dimension was plotted against time. Time 0 represents initial induction with doxycycline. Red brackets, periods during which the animal was on doxycycline induction; blue lines, periods without doxycycline administration. Insets: Representative photographs of R348 tumour taken at times shown (on and 12 days off) during the first cycle of doxycycline treatment. All primary melanomas ($n = 10$) regressed rapidly following doxycycline withdrawal, although two of the largest tumours recurred at the site as slow-growing tumours of indeterminate type (see text). Two fully regressed tumour-bearing mice were re-induced to form large tumours, one of which regressed fully after doxycycline withdrawal (shown here), and the other showed stable growth for 10 more days before being killed. **B**, Regression of primary melanoma in R767. **a**, on; **b**, 3 days off; **c**, 10 days off. **C**, Haematoxylin and eosim-stained sections of one of the tumours in R348 measured and shown in **A**. Top panel, 200×, and lower panel, 400× original magnification. On, histology of the tumour biopsied while on doxycycline. Note anaplastic and pleiomorphic large cells. 48 h off, histology of the tumour biopsed 48 h after withdrawal of doxycycline. Note more orderly spindle morphology. 12 day off, histology of the site where tumour was biopsied 12 days after withdrawal of doxycycline. Note intact epidermis and scattered foci of transformed cells (arrows). Asterisk, hair follicle; e, epidermis. **D**, top, TUNEL staining of tumours from mouse R405 (Tet–Ras founder line 72) biopsied on (left) and 72 h off doxycycline (middle); right, higher-power magnification of the bracketed region in middle (arrow, TUNEL positivity in endothelial cell); middle, Ki67 immunostaining for detection of S-phase nuclei; bottom, anti-CD34 staining in the same tissues.

melanomas[5], manifesting as amelanotic, invasive and highly vascular tumours—features that are reminiscent of nodular-type melanoma in humans (for example, see Fig. 2A, B). Histological examination revealed a spindle morphology with anaplastic and pleiomorphic cytology (Fig. 2C), strong immunoreactivity to the early melanocyte-specific marker tyrosinase-related-protein-1 (TRP-1)[6], and robust H-Ras^{V12G} expression and activity in tumours and tumour-derived cell lines in culture (Figs 1b and 4a).

Although these and previous results[5,7] confirm a causal role for H-Ras^{V12G} in melanoma development, the ability to regulate H-Ras^{V12G} activity in these melanomas allowed us to determine the role of activated Ras in tumour maintenance. To this end, different doxycycline-treated Tyr/Tet–Ras INK4a$^{-/-}$ mice with one or more independent primary melanomas, ranging in size from 0.5 to 1.5 cm in diameter, had doxycycline administration withdrawn (Fig. 2A, B). Following an initial loss of tumour erythema (Fig. 2B, compare b to a), these large tumours regressed to barely detectable or undetectable lesions with only residual scattered tumour foci on microscopic examination by day 14 of doxycycline withdrawal (Fig. 2C, compare right panel with left). Consistent with the presence of residual microscopic disease, re-administration of doxycycline resulted in the rapid recurrence of tumours at previous tumour sites (Fig. 2A). This model may be useful in the development of anti-oncologics directed towards minimal residual disease. All primary melanomas ($n = 10$) exhibited regression upon doxycycline withdrawal; however, doxycycline-independent tumours can persist or re-emerge ($n = 3$), particularly with large tumour burdens (Fig. 2). These later tumours were whitish, exhibited a less anaplastic spindle cytology, failed to express the H-Ras^{V12G} transgene (by western blot analysis) and were TRP-1 negative (data not shown). These data indicate that these doxycycline-independent tumours are either a different cancer type, such as fibrosarcoma, or Ras-independent melanomas.

Although these results and those of others[8] confirm a role for Ras in tumorigenesis, this model system allows us to investigate mechanisms underlying tumour regression *in vivo*. We first assessed the impact of doxycycline withdrawal in different Tyr/Tet–Ras INK4a$^{-/-}$ tumour-derived cell lines in cell culture. Melanoma cell lines were established from primary tumours in doxycycline-supplemented medium and were shown to express H-Ras^{V12G} messen-

A

With doxycycline | Without doxycycline

Cell line	With doxycycline No. SCID	Tumour	Without doxycycline No. SCID	Tumour	Duration
R192	4	4	2	0	4.5
R405	3	3	1	0	1.5
R545	28	28	2	0	4.0
R767	20	20	1	0	3.0

B

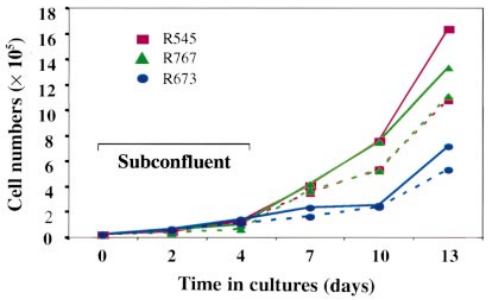

Figure 3 *In vitro* and *in vivo* behaviour of melanoma cells in the presence and absence of doxycycline. **A**, Photomicrograph of SCID mice maintained on (**a**) and off (**b**) doxycycline after subcutaneous injection of R192 cells. Arrows, subcutaneous tumours. Similar experiments performed with multiple independently derived melanoma cell lines are summarized in the table. 'Duration' refers to the period of observation in months. **B**, Growth-curves of three independently derived melanoma cell lines with and without doxycycline supplementation in medium (see Methods). Solid lines, doxycycline-treated; dotted lines, doxycycline-free. Cultures were subconfluent during the first 5 days.

ger RNA, protein, and activity in a doxycycline-dependent manner (Fig. 4a and data not shown). The derivative melanoma cell lines remained doxycycline-responsive, as shown by their strict doxycycline-dependency for tumorigenic potential in severe-combined immunodeficient (SCID) mice. Specifically, subcutaneous injection of purified Tyr/Tel–Ras INK4a$^{-/-}$ melanoma cell lines yielded tumours in SCID mice treated with doxycycline with 100% efficiency, whereas those mice not receiving doxycycline remained tumour-free after many months of observation (Fig. 3A). In cell culture, the presence or absence of doxycycline did not significantly influence the subconfluent growth rates of multiple independently derived lines (Fig. 3B). Similarly, the presence of doxycycline did not confer enhanced growth potential in low-serum conditions (0.5 and 1% FCS; data not shown). However, the presence of doxycycline slightly enhanced growth in dense cultures, indicating that *in vivo* Ras expression may provide a continued cell-autonomous advantage for tumour growth. On the other hand, the data is also consistent with the possibility that tumour regression following doxycycline withdrawal may reflect a continued requirement for Ras in promoting and sustaining non-cell-autonomous tumour–host interactions that are essential for tumour growth and maintenance.

One hypothesis supporting the latter possibility is that continued expression of Ras confers on the tumour cells the capacity to evade the host immune response[9]; thus, tumour regression is due to onset of immune rejection by the host. To examine the contribution of an intact immune system to tumour regression, we determined the regression kinetics of tumours derived from purified Tyr/Tet–Ras INK4a$^{-/-}$ melanoma cell lines in SCID tumour explants. Upon doxycycline withdrawal, established tumours showed rapid reductions in tumour size accompanied by histological, proliferative and apoptotic profiles that were indistinguishable from those of the primary tumours in immune-competent hosts (data not shown). As SCID mice lack functioning B and T lymphocytes (although they have functional natural killer cells and macrophages), these data are consistent with the view that the immune system is not critical during the initial phase in which the bulk of the tumour burden is eliminated.

Another important aspect of tumour reliance on host interactions involves angiogenic support. In fact, examination of regressing tumours indicated that vascular regression might even precede frank tumour loss. We performed serial biopsies of the same primary Tyr/Tet–Ras INK4a$^{-/-}$ tumours following doxycycline withdrawal at 0, 24, 48 and 72 h. Tumour-bearing mice from Tet–Ras founder lines 65 and 72 were examined (for example, R348 and R405 from line 65 and 72, respectively) and yielded identical phenotypes. Upon microscopic examination, a morphological transition from severe anaplasia to a more organized spindle cytoarchitecture occurred by 48 h after doxycycline withdrawal (R348 tumour shown in Fig. 2C). A slight decline in proliferative index and a marked increase in apoptosis (R405 tumour shown in Fig. 2D) accompanied these histological changes. In many primary tumours that we examined, the apoptotic response was evident as early as 24 h after doxycycline withdrawal (data not shown). Most notably, many TUNEL-positive cells were found in close proximity to small tumour vessels, specifically the cells comprising the vessel wall (Fig. 2D). Vessel-associated apoptosis coincided with a marked decrease in immunoreactivity for CD34 and CD31, two classical endothelial-cell markers[10,11] (Fig. 2D; CD31 not shown).

The significant apoptotic rate of cells lining tumour vessels suggested that continued activated-Ras expression may be required for the critical host–tumour symbiotic interaction that sustains stable tumour vasculature. Consistent with this, previous cell-culture data have shown that oncogenic K- and H-Ras^{V12G} can stimulate VEGF expression[12–14]. To determine the role, if any, of VEGF in Ras-dependent tumour maintenance, Ras activity (as measured by the Raf–GST pull-down assay) and VEGF protein level (see Methods) were serially determined in cell culture and tumour explants following doxycycline withdrawal. In cell culture, a decline in H-Ras^{V12G} activity correlated with downregulation of VEGF expression (Fig. 4a, b). In the tumour explants, although a decline in Ras activity led to an eventual decrease in VEGF during later stages of tumour regression (after day 3; Fig. 4a, b), early regression and endothelial-cell apoptosis occurred despite sustained VEGF expression (Fig. 4c, d), presumably due to hypoxic/anoxic stimuli[15–18]. The contrasting VEGF kinetics indicated that tumour regression *in vivo* is not mediated by the loss of Ras-stimulated VEGF expression and that high VEGF levels are insufficient to maintain tumour viability in the absence of H-Ras^{V12G} expression. To examine this issue more directly, the doxycycline-responsive R545 melanoma cell line was engineered to constitutively express either GFP (green fluorescent protein) or VEGF with GFP. The VEGF-transduced cell lines expressed on average 10 times more VEGF than the GFP-transduced control in the absence of doxycycline (10 ng ml^{-1} versus $<$1 ng ml^{-1} by ELISA). Although the VEGF-transduced cells showed faster tumour growth, withdrawal of doxycycline resulted in regression of these tumours, despite enforced VEGF expression (Fig. 4c). Furthermore, as in primary tumours and SCID tumours derived from the parental untransduced melanoma lines, this tumour regression was associated with marked activation of apoptosis in tumour cells and in host endothelial cells (Fig. 4d).

Together, these data show that, although activated Ras regulates VEGF expression in tumour cells as previously reported[13,19–21], complex and poorly understood Ras-independent mechanisms

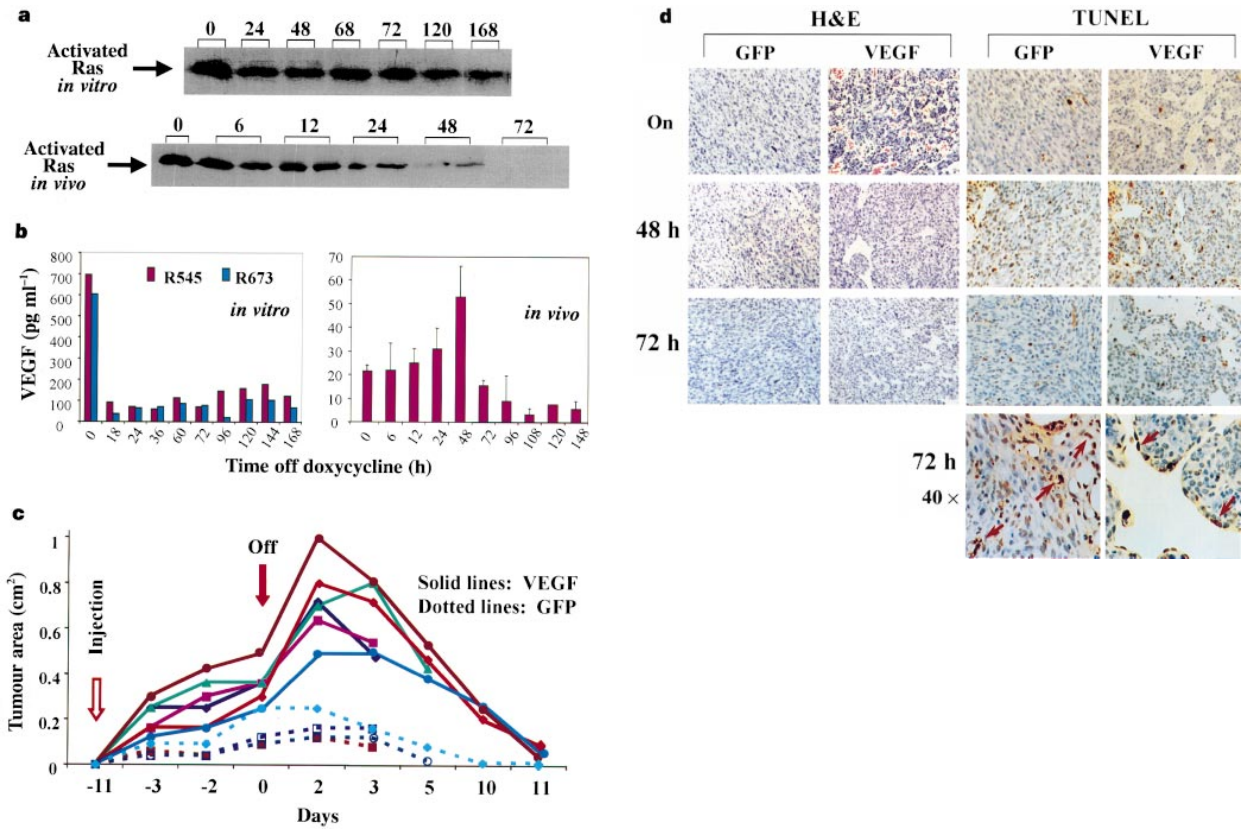

Figure 4 VEGF is not sufficient to sustain tumour viability following doxycycline withdrawal. **a**, Ras activity after withdrawal from doxycycline *in vivo* and *in vitro*. R545 melanoma cells in cultures or R545-derived SCID tumours were subjected to Raf–GST pull-down assay (see Methods) to determine Ras activity at indicated time after doxycycline withdrawal. For *in vivo* assay, two independently derived samples were assayed except for the 0 h time-point. **b**, Endogenous VEGF protein in cultured R545 and R673 cells (left) and SCID-derived R545 tumours (right). **c**, Enforced VEGF expression in R545 melanoma cells is not sufficient to block tumour regression in SCID mice after doxycycline withdrawal. Transduced cells were injected on day –11 and doxycycline was withdrawn from drinking water on day 0. **d**, Haematoxylin and eosin (H&E) and TUNEL staining of SCID tumours from **C**. Note large ectactic vascular spaces in VEGF-transduced tumours. Increase in number of TUNEL-positive nuclei (both tumour and endothelial cells) was evident both 48 h and 72 h after doxycycline withdrawal in tumours with or without enforced VEGF expression. Arrows, TUNEL-positive endothelial cells lining vascular spaces.

contribute significantly to the regulation of VEGF in established tumours upon doxycycline withdrawal. Correspondingly, the fact that initiation of tumour regression and associated vascular collapse take place despite either robust endogenous or retrovirally enforced VEGF expression indicates that VEGF is not sufficient for tumour maintenance, consistent with previous findings[14], and that the role of activated Ras in tumour maintenance extends beyond the regulation of VEGF expression. Thus, the *in vivo* model reported here will serve to uncover additional aspects of the complex homotypic and heterotypic interactions between host and tumour cells that are essential for the maintenance of fully formed solid tumours. Whereas an improved understanding of such interactions could stimulate the development of therapeutics directed towards the less plastic host-cell compartment, it is notable that despite the occurrence of many genetic changes in these tumours, effective anti-Ras therapeutics would be predicted to hold significant promise in anticancer therapy. □

Methods

Production of the transgenic mice. The reverse tetracycline transactivator (rtTA) is a 1,050-base pair (bp) *Eco*RI/*Bam*HI fragment isolated from pUHD172-1neo[2]. The Tet promoter contains an *Xho*I/*Eco*RI fragment of the cytomegalovirus minimal promoter linked to the tet operator sequences[2]. The tyrosinase enhancer/promoter and the H-Ras^{Val12} transgene were as described[3,5,22]. We generated multiple founder lines for both transgenes at the expected frequencies. We used one activator line (Tyr/rtTA, line 37) and two independent reporter lines (Tet-RAS, lines 65 and 72) for these studies.

Primary tumours, derivative cell lines and SCID explant tumours. Transgenic mice were fed doxycycline drinking water (2 mg ml^{-1} in sucrose water) and observed for spontaneous tumour development. Primary tumours were adapted to culture by mechanical mincing with sterilized razor blades and brief trypsinization, and maintained in RPMI medium containing 10% serum and supplemented with doxycycline (2 μg ml^{-1} medium)[4]. For the SCID explant tumours, 2–5 × 10^6 established melanoma cells were injected subcutaneously into the flanks of adult SCID mice maintained on doxycycline or regular drinking water. These cell lines were passaged sufficiently to insure elimination of immunocytes from the original host.

RNA and protein analysis. Total RNAs were isolated from tumour tissues and cells using Trizol reagents (Gibco BRL). For H-Ras^{V12G}, a 700-bp *Sal*I complementary DNA fragment isolated from pBABE-Ras (a gift from S. Lowe) was used as a probe. For VEGF, a *Sac*I/*Kpn*1 600-bp ORF fragment was isolated from mouse VEGF plasmid (a gift from P. Maisonpierre). RNA *in situ* hybridization was performed as described[23] on tumour samples snap-frozen in OCT (Lab-Tek). Western blots of tumour or cell lysates (100 μl input) were run on 15% SDS–PAGE and probed with anti-Ras monoclonal antibodies (Oncogene). Ras activity was determined by a Ras activation assay (Upstate Biotechnology), following the manufacturer's protocol. VEGF protein levels were determined in duplicate by ELISA (R&D System) using 100 μg of protein (from tissue lysates or conditioned media). Microplates were read using the OPTIMax tunable microplate reader (Molecular Devices) and analysed with SoftMax Pro.

Histological analysis and immunohistochemistry. Tissue samples were formalin-fixed and paraffin-embedded. Anti-TRP1 staining using a TA99

monoclonal antibody[6], TUNEL staining, Ki67 and anti-CD34 staining were performed as described[5,11,24,25].

Growth curves. Cells from each cell line were seeded at a density of 20,000 cells per well in a 12-well plate in medium with or without doxycycline. Medium was changed every 3 days for all samples. Duplicate wells were trypsinized, and cell numbers were counted by haemacytometer at indicated time points and plotted against time. Studies were conducted in media containing 10, 1 and 0.5% serum. Growth-curve determinations were performed in cells maintained on doxycycline before experiments as well as onset of cells that had been removed from doxycycline for 3 days before the experiments.

Enforced VEGF-expressing melanoma cell line. The R545 melanoma cell line was transduced with LZRSpBMN–IRES–GFP and LZRSpBMN–VEGF–IRES–GFP, and purified populations were established by FACS sorting[26]. SCID explant experiments used transduced cell lines generated as described above. Tumour sizes were measured with tumour callipers in two dimensions and area plotted against time (in days).

Received 19 March; accepted 22 June 1999.

1. Bishop, J. M. Molecular themes in oncogenesis. *Cell* **64,** 235–248 (1991).
2. Gossen, M. *et al.* Transcriptional activation by tetracyclines in mammalian cells. *Science* **268,** 1766–1769 (1995).
3. Fasano, O., Taparowsky, E., Fiddes, J., Wigler, M. & Goldfarb, M. Sequence and structure of the coding region of the human H-ras-1 gene from T24 bladder carcinoma cells. *J. Mol. Appl. Genet.* **2,** 173–180 (1983).
4. Kistner, A. *et al.* Doxycycline-mediated quantitative and tissue-specific control of gene expression in transgenic mice. *Proc. Natl Acad. Sci. USA* **93,** 10933–10938 (1996).
5. Chin, L. *et al.* Cooperative effects of *INK4a* and *ras* in melanoma susceptibility *in vivo*. *Genes Dev.* **11,** 2822–2834 (1997).
6. Thomson, T. M. *et al.* Differentiation antigens of melanocytes and melanoma: analysis of melanosome and cell surface markers of human pigmented cells with monoclonal antibodies. *J. Invest. Dermatol.* **90,** 459–466 (1988).
7. Gause, P. R. *et al.* Chromosomal and genetic alterations of 7,12-dimethylbenz[a]anthracene-induced melanoma from TP-ras transgenic mice. *Mol. Carcin.* **20,** 78–87 (1997).
8. Shirasawa, S., Furuse, M., Yokoyama, N. & Sasazuki, T. Altered growth of human colon cancer cell lines disrupted at activated Ki-ras. *Science* **260,** 85–88 (1993).
9. Doherty, P. C., Tripp, R. A. & Sixbey, J. W. Evasion of host immune responses by tumours and viruses. *Ciba Found. Symp.* **187,** 245–256 (1994).
10. Bird, I. N., Spragg, J. H., Ager, A. & Matthews, N. Studies of lymphocyte transendothelial migration: analysis of migrated cell phenotypes with regard to CD31 (PECAM-1), CD45RA and CD45RO. *Immunology* **80,** 553–560 (1993).
11. Traweek, S. T., Kandalaft, P. L., Mehta, P. & Battifora, H. The human hematopoietic progenitor cell antigen (CD34) in vascular neoplasia. *Am. J. Clin. Pathol.* **96,** 25–31 (1991).
12. Rak, J. *et al.* Oncogenes as inducers of tumor angiogenesis. *Cancer Metastasis Rev.* **14,** 263–277 (1995).
13. Arbiser, J. L. *et al.* Oncogenic H-ras stimulates tumor angiogenesis by two distinct pathways. *Proc. Natl Acad. Sci. USA* **94,** 861–866 (1997).
14. Okada, F. *et al.* Impact of oncogenes in tumor angiogenesis: mutant K-ras up-regulation of vascular endothelial growth factor/vascular permeability factor is necessary, but not sufficient for tumorigenicity of human colorectal carcinoma cells. *Proc. Natl Acad. Sci. USA* **95,** 3609–3614 (1998).
15. Shweiki, D., Itin, A., Soffer, D. & Keshet, E. Vascular endothelial growth factor induced by hypoxia may mediate hypoxia-initiated angiogenesis. *Nature* **359,** 843–845 (1992).
16. Mazure, N. M., Chen, E. Y., Yeh, P., Laderoute, K. R. & Giaccia, A. J. Oncogenic transformation and hypoxia synergistically act to modulate vascular endothelial growth factor expression. *Cancer Res.* **56,** 3436–3440 (1996).
17. Goldberg, M. A. & Schneider, T. J. Similarities between the oxygen-sensing mechanisms regulating the expression of vascular endothelial growth factor and erythropoietin. *J. Biol. Chem.* **269,** 4355–4359 (1994).
18. Mukhopadhyay, D. *et al.* Hypoxic induction of human vascular endothelial growth factor expression through c-Src activation. *Nature* **375,** 577–581 (1995).
19. Rak, J. *et al.* Mutant ras oncogenes upregulate VEGF/VPF expression: implications for induction and inhibition of tumor angiogenesis. *Cancer Res.* **55,** 4575–4580 (1995).
20. Grugel, S., Finkenzeller, G., Weindel, K., Barleon, B. & Marme, D. Both v-Ha-Ras and v-Raf stimulate expression of the vascular endothelial growth factor in NIH 3T3 cells. *J. Biol. Chem.* **270,** 25915–25919 (1995).
21. Larcher, F. *et al.* Up-regulation of vascular endothelial growth factor/vascular permeability factor in mouse skin carcinogenesis correlates with malignant progression state and activated H-ras expression levels. *Cancer Res.* **56,** 5391–5396 (1996).
22. Ganss, R., Montoliu, L., Monaghan, A. P. & Schutz, G. A cell-specific enhancer far upstream of the mouse tyrosinase gene confers high level and copy number-related expression in transgenic mice. *EMBO J.* **13,** 3083–3093 (1994).
23. Valenzuela, D. M. *et al.* Receptor tyrosine kinase specific for the skeletal muscle lineage: expression in embryonic muscule, at the neuromuscular junction, and after injury. *Neuron* **15,** 573–584 (1995).
24. Schreiber-Agus, N. *et al.* Role of Mxi1 in ageing organ systems and the regulation of normal and neoplastic growth. *Nature* **393,** 483–487 (1998).
25. Gavrieli, Y., Sherman, Y. & Ben-Sasson, S. A. Identification of programmed cell death *in situ* via specific labeling of nuclear DNA fragmentation. *J. Cell Biol.* **119,** 493–501 (1992).
26. Cheng, L., Fu, J., Tsukamoto, A. & Hawley, R. G. Use of green fluorescent protein variants to monitor gene transfer and expression in mammalian cells. *Nature Biotech.* **14,** 606–609 (1996).

Acknowledgements. We thank G. Schutz for the tyrosinase promoter–enhancer elements; S. Jiao for tissue sample processing and immunohistochemistry; D. Compton for RNA *in situ* hybridization, and M. Russell for technical assistance. This work was supported by an NIH Mentored Clinician Scientist Award and the Harvard Skin Disease Center Grant (L.C.); by grants from the NIH (C.C.C. and R.A.D.) and from the DFCI Cancer Core (R.A.D. and L.C.). R.A.D. is an American Cancer Society Research Professor; A.T. and J.P. are HHMI Medical Student Fellows.

Correspondence and requests for materials should be addressed to R.A.D. (e-mail: ron_depinho@dfci.harvard.edu) or L.C. (e-mail: lynda_chin@dfci.harvard.edu).

Structure of the C-terminal domain of FliG, a component of the rotor in the bacterial flagellar motor

Scott A. Lloyd*‡, Frank G. Whitby†‡, David F. Blair* & Christopher P. Hill†

* *Department of Biology, University of Utah, 257 South 1400 East, Salt Lake City, Utah 84112-0840, USA*
† *Department of Biochemistry, University of Utah, 50 North Medical Drive, Salt Lake City, Utah 84132, USA*
‡ *These authors contributed equally to this work*

Many motile species of bacteria are propelled by flagella, which are rigid helical filaments turned by rotary motors in the cell membrane[1–3]. The motors are powered by the transmembrane gradient of protons or sodium ions. Although bacterial flagella contain many proteins, only three—MotA, MotB and FliG—participate closely in torque generation. MotA and MotB are ion-conducting membrane proteins that form the stator of the motor. FliG is a component of the rotor, present in about 25 copies per flagellum. It is composed of an amino-terminal domain that functions in flagellar assembly and a carboxy-terminal domain (FliG-C) that functions specifically in motor rotation. Here we report the crystal structure of FliG-C from the hyperthermophilic eubacterium *Thermotoga maritima*. Charged residues that are important for function, and which interact with the stator protein MotA[4,5], cluster along a prominent ridge on FliG-C. On the basis of the disposition of these residues, we present a hypothesis for the orientation of FliG-C domains in the flagellar motor, and propose a structural model for the part of the rotor that interacts with the stator.

We used FliG and FliG-C proteins from *Escherichia coli* for initial crystallization trials, because extensive mutational studies have been done using this species and the closely related species *Salmonella typhimurium*[4,6]. Purified FliG and FliG-C from *E. coli* were polydisperse and failed to crystallize, however, which prompted us to study the protein from the hyperthermophile *T. maritima*[7]. The amino-acid sequence of *T. maritima* FliG-C (residues 209–335) is 46% identical to the protein from *E. coli* (Fig. 1), and charge is conserved at the functionally important positions. Null *fliG* mutants of *E. coli* are non-flagellate because FliG is required for flagellar assembly as well as rotation[8]. Both flagellar assembly and motility were restored to this mutant by a plasmid expressing a chimaeric protein consisting of residues 1–240 of *E. coli* FliG (the domain required for flagellar assembly) fused to residues 243–335 of *T. maritima* FliG (the domain required for rotation). Thus, the bulk of the FliG domain studied here is functionally interchangeable with the corresponding part of the *E. coli* protein. A plasmid that expressed full-length *T. maritima* FliG did not restore flagella to the mutant, presumably because the N-terminal domain of the *T. maritima* protein did not interact properly with other flagellar proteins of *E. coli*.

We overexpressed and purified full-length *T. maritima* FliG, but dynamic light scattering showed this to be highly polydisperse. A C-terminal domain consisting of residues 209–335 was found to be monodisperse. This domain was crystallized and its structure was determined by multiwavelength anomalous diffraction (MAD) and refined at 2.2 Å resolution to an *R*-factor (R_{free}) of 23.6% (30.4%) (Tables 1 and 2). The ordered residues (235–335) form a compact domain comprising six helices[9] folded into a roughly triangular prism of approximate dimensions 38 Å × 30 Å × 27 Å (Figs 1 and